Progress in Microbes and Molecular Biology

HH PUBLISHER

Original Research Article

Exploratory Analysis of Ferroptosis-Related DNA Methylation in Colorectal Cancer Identifies Candidate Tissue-Discriminatory and Survival-Associated Loci

Fam Mei Kei[1], Muhammad Redha Abdullah Zawawi[2], Habsah Aziz[3], Loh Teng-Hern Tan[4,5,6], Jodi Woan-Fei Law[4,5,6], Nurul Syakima Ab Mutalib[7*]

Article History

Received: 13 September 2026;

Received in Revised Form: 03 November 2025;

Accepted: 18 November 2026;

Available Online: 25 November 2026

[1]Department of Biomedical Sciences, Center for Toxicology and Health Risk Studies, Faculty of Health Sciences, Universiti Kebangsaan Malaysia, Jalan Raja Muda Abdul Aziz, 50300 Kuala Lumpur, Federal Territory of Kuala Lumpur, Malaysia; a182700@siswa.ukm.edu.my (FMK)

[2]UKM Medical Molecular Biology Institute (UMBI), Universiti Kebangsaan Malaysia, Jalan Yaacob Latiff, Bandar Tun Razak, 56000 Cheras, Kuala Lumpur, Malaysia; mraz@ukm.edu.my (MRAZ)

[3]Institute of Systems Biology, Universiti Kebangsaan Malaysia, 43600 Bangi, Selangor, Malaysia; habsah@ukm.edu.my (HA)

[4]RII Centre for Molecular and Microbiome Sciences, Research Innovation Institute (RII), University of Nottingham Ningbo China, Ningbo 315000, China; loh-teng-hern.tan@nottingham.edu.cn (LTHT), Jodi-Woan-Fei.Law@nottingham.edu.cn (JWFL)

[5]School of Health and Life Sciences, University of Nottingham Ningbo China, Ningbo 315000, China

[6]Microbiome and Bioresource Research Strength (MBRS), Jeffrey Cheah School of Medicine and Health Sciences, Monash University Malaysia, Bandar Sunway 47500, Selangor Darul Ehsan, Malaysia

[7]Department of Biological Science and Biotechnology, Faculty of Science and Technology, Jalan Nik Ahmed Kamil, Universiti Kebangsaan Malaysia, 43600 Bangi, Selangor, Malaysia

*Corresponding author: Nurul Syakima Ab Mutalib; Department of Biological Science and Biotechnology, Faculty of Science and Technology, Jalan Nik Ahmed Kamil, Universiti Kebangsaan Malaysia, 43600 Bangi, Selangor, Malaysia; syakima@ukm.edu.my (NSAM)

Abstract: Colorectal cancer (CRC) is characterised by extensive epigenetic dysregulation, while ferroptosis is increasingly recognised as an important regulator of tumour biology and treatment response. However, locus-specific DNA methylation alterations affecting ferroptosis-related genes in CRC remain poorly characterised. This exploratory secondary analysis investigated locus-specific DNA methylation across curated ferroptosis-driver and ferroptosis-suppressor genes and evaluated their functional context, exploratory survival signals and apparent tissue-discriminatory potential. Infinium HumanMethylation450K data from 54 CRC tissues and 54 paired adjacent-normal colon tissues were re-analysed.

Differentially methylated probes (DMPs) were defined using a Benjamini-Hochberg-adjusted P<0.05 and |Δβ|≥0.20 and mapped to ferroptosis-related genes from FerrDb V2. Functional enrichment was performed using GeneCodis 4/BioPlanet, survival associations were explored using MethSurv in TCGA colon adenocarcinoma (COAD) and rectal adenocarcinoma (READ), and tissue-discriminatory potential was assessed by receiver operating characteristic analysis. Fifty-five DMPs across 38 ferroptosis-related genes were identified, comprising 35 DMPs in 24 driver genes and 20 DMPs in 14 suppressor genes. Of these, 53/55 (96.4%) were hypomethylated and two were hypermethylated. Ferroptosis-driver genes were significantly enriched in the ATF2 transcription factor network (5 genes; adjusted $P=8.5\times10^{-5}$) and autophagy regulation (4 genes; adjusted $P=1.16\times10^{-4}$), whereas ferroptosis-suppressor genes were enriched in p53 signalling (4 genes; adjusted $P=3.14\times10^{-3}$) and the Keap1-NRF2 pathway (2 genes; adjusted $P=6.66\times10^{-3}$). Eight DMPs across *CDO1*, *DNAJB6*, *MAPK14*, *MAPK9* and *CAV1* met the prespecified exploratory LR-test P<0.05 threshold, without correction for multiple testing. *DNAJB6* cg27023755 met this exploratory threshold in both COAD (P=0.029) and READ (P=0.044). *SNX4* cg27440834 showed the highest apparent tissue-discriminatory AUC in the discovery dataset (AUC=0.9300; 95% CI 0.8834–0.9766; P<0.0001). These exploratory findings identify locus-specific ferroptosis-related methylation alterations in CRC and prioritise candidate CpG loci for independent validation, functional investigation and future evaluation in clinically accessible specimens.

Keywords: Colorectal cancer; DNA methylation; ferroptosis; epigenetics; biomarker; SDG 3 Good health and well-being

1. Introduction

Colorectal cancer (CRC) is one of the most common malignancies worldwide. Global estimates indicate that approximately 1.9 million new CRC cases occurred in 2020 and that the burden may rise substantially by 2040 [1]. In Malaysia, CRC is a major cause of cancer morbidity and mortality, with particularly high incidence among men and women [2]. CRC is molecularly heterogeneous, with genomic alterations and affected pathways varying according to tumour location [3]. Beyond recurrent genetic alterations, CRC development is also shaped by epigenetic dysregulation, including aberrant DNA methylation [4–9].

DNA methylation, most commonly involving methylation of cytosine at CpG dinucleotides, contributes to transcriptional regulation and maintenance of normal cellular identity. Aberrant hypermethylation or hypomethylation can disrupt gene regulation in cancer and may provide stable molecular signals with diagnostic, prognostic or therapeutic relevance [10,11]. Because epigenetic alterations are potentially reversible, defining disease-associated methylation changes may also provide mechanistic insight into pathways that are not fully explained by somatic mutation alone.

Ferroptosis is an iron-dependent, non-apoptotic form of regulated cell death first defined by Dixon and colleagues [12]. It is characterised by intracellular iron accumulation, oxidative stress and lipid peroxidation and is regulated through interconnected systems including system xc-/glutathione/GPX4, iron metabolism, lipid metabolism, p53 signalling and ferroptosis-suppressor mechanisms [13,14]. Ferroptosis is increasingly recognised as relevant to CRC biology and treatment response [15]. Importantly, epigenetic regulation can influence genes involved in ferroptosis, suggesting that DNA methylation may alter the ferroptotic state of cancer cells [16].

Ferroptosis-associated DNA methylation signatures have been explored in several tumour types, but their role in CRC remains comparatively underexplored. Much of the recent CRC literature has focused on ferroptosis-related gene-expression signatures and prognostic models, as well as regulatory mechanisms involving non-coding RNAs and other post-transcriptional processes [17,18]. One recent CRC ferroptosis study also examined DNA methylation of three selected genes, reporting altered CpG and promoter methylation involving *GPX3*, *CDKN2A* and *SLC7A11* [17]. However, that analysis was restricted to genes selected from an expression-based prognostic signature and did not systematically interrogate CpG-level methylation across a curated ferroptosis-regulator set. Thus, the locus-specific DNA methylation landscape of ferroptosis drivers and suppressors in CRC remains incompletely characterised. Recent work has also highlighted extensive interactions between miRNAs, lncRNAs and circRNAs and ferroptosis-related pathways in CRC, including their potential prognostic and therapeutic relevance [19]. By comparison, systematic CpG-level characterisation of DNA methylation across curated ferroptosis-driver and ferroptosis-suppressor genes in CRC remains limited. The present study therefore re-analysed an existing CRC methylation dataset to identify differentially methylated ferroptosis-related loci, define their functional pathway context, and evaluate their survival associations and tissue-discriminatory potential.

2. Materials and Methods

2.1. Study Design and Tissue Dataset

This study was designed as a secondary integrative analysis. The methylation dataset was derived from previously published methylome profiling of 54 CRC tumours and 54 matched adjacent-normal tissues using the Infinium HumanMethylation450 BeadChip (GEO accession GSE193535; n=108) [20]. In that work, genomic DNA was extracted from pathologist-reviewed tissue, subjected to bisulfite conversion and profiled using the Infinium HumanMethylation450 BeadChip. The array interrogated 485,577 CpG loci. The present study involved secondary analysis of existing data and did not involve additional participant recruitment or specimen collection.

2.2. DNA Extraction, Bisulfite Conversion and 450K Methylation Profiling

DNA was extracted using the QIAamp DNA Mini Kit (Qiagen, USA). DNA quantity and purity were assessed using a Qubit 2.0 fluorometer and NanoDrop 2000c spectrophotometer (Thermo Fisher Scientific, USA), respectively; samples with a purity ratio of 1.8-2.0 were retained. A total of 500 ng DNA was subjected to bisulfite conversion using the EZ DNA Methylation-Gold Kit (Zymo Research, USA). Genome-wide DNA methylation was profiled using the Infinium HumanMethylation450 BeadChip (Illumina, USA), which interrogates approximately 485,000 CpG loci.

Methylation data were processed using GenomeStudio v2.0.4 and the ChAMP [21] Bioconductor workflow. CpG loci with detection P>0.01 were excluded, and raw intensities were processed using Peak-Based Correction (PBC), followed by ComBat batch correction [22,23]. DMPs were annotated using the standard IlluminaHumanMethylation450kanno.ilmn12.hg19 annotation implemented in the ChAMP workflow, and the resulting gene annotations were used to match significant probes against the FerrDb V2 ferroptosis-driver and ferroptosis-suppressor gene sets. Beta values were extracted for downstream analysis. Differential methylation was assessed using limma-based statistics with Benjamini-Hochberg correction. CpGs with adjusted $P<0.05$ and delta-beta ≥ 0.20 were classified as hypermethylated, whereas CpGs with delta-beta ≤ -0.20 were classified as hypomethylated in tumour relative to adjacent-normal tissue.

2.3. Ferroptosis Gene Annotation and Differentially Methylated Probe Mapping

Ferroptosis-driver and ferroptosis-suppressor genes were obtained from FerrDb V2, the updated manually curated resource of ferroptosis regulators and disease associations [24]. The FerrDb v2 lists comprised 369 driver annotations and 348 suppressor annotations, with 264 unique driver genes and 238 unique suppressor genes. Differentially methylated probes (DMPs) were mapped to their gene annotations as generated by the methylation-analysis pipeline and subsequently filtered against the FerrDb V2 ferroptosis-driver and ferroptosis-suppressor gene sets. In the resulting DMP output, each annotated CpG probe was assigned to a single gene; no probes with multiple gene assignments were observed. Gene feature and CpG island context annotations were retained for downstream interpretation. The analytical workflow used in this study is summarised in Figure 1.

2.4. Functional Enrichment Analysis

Differentially methylated ferroptosis-driver and ferroptosis-suppressor gene sets were analysed separately using GeneCodis 4 [25,26] with the BioPlanet pathway resource. Pathways with adjusted $P<0.05$ were considered significantly enriched. Relative enrichment scores generated by the platform were used to support interpretation and ranking of enriched pathways.

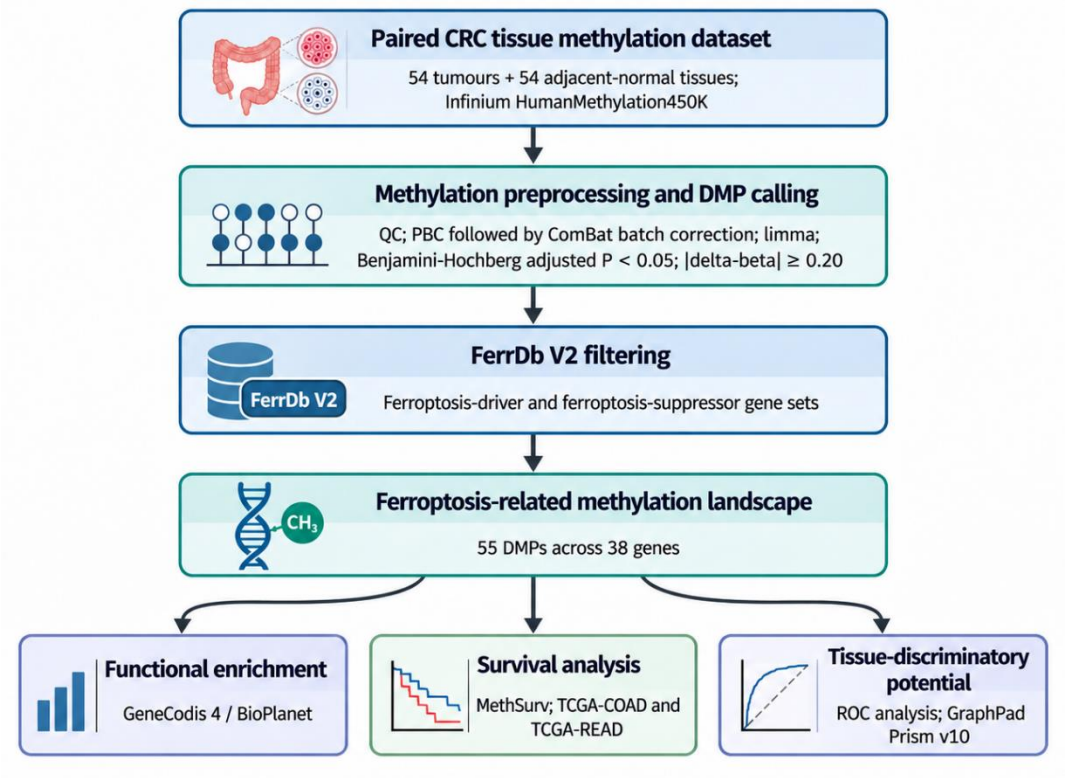


Figure 1. Analytical workflow for identifying differentially methylated ferroptosis-related loci in colorectal cancer and evaluating their functional enrichment, survival associations and tissue-discriminatory potential. CRC, colorectal cancer; DMP, differentially methylated probe; PBC, Peak-Based Correction; TCGA-COAD, The Cancer Genome Atlas colon adenocarcinoma cohort; TCGA-READ, The Cancer Genome Atlas rectal adenocarcinoma cohort; ROC, receiver operating characteristic.

2.5. Survival Analysis

Associations between individual ferroptosis-related DMPs and patient survival were explored using MethSurv, a web-based survival-analysis resource based on TCGA Infinium HumanMethylation450K methylation data [27]. Kaplan–Meier analyses were performed independently in The Cancer Genome Atlas colon adenocarcinoma (TCGA-COAD) and rectal adenocarcinoma (TCGA-READ) datasets. Patients were stratified into higher- and lower-methylation groups using the MethSurv "best cut-off point" procedure, which selects the cut-off yielding the highest hazard ratio from mean, median, lower-quartile, upper-quartile and MAXSTAT-based thresholds. Analyses were performed without adjustment for clinical covariates. Because the survival analysis was intended as hypothesis-generating screening, no multiple-testing correction was applied across the unique CpG probes tested. An LR-test $P<0.05$ was therefore used as a prespecified exploratory threshold rather than as confirmatory evidence of prognostic association.

2.6. Tissue-Discriminatory Potential

The tissue-discriminatory potential of the 55 ferroptosis-related DMPs was evaluated by ROC analysis using GraphPad Prism v10 (GraphPad Software, USA). Area under the ROC curve (AUC), standard error, 95% confidence interval (CI) and P value were calculated

by comparing tumour and paired adjacent-normal methylation values. AUC values above 0.90 were interpreted as indicating excellent discrimination.

3. Results

3.1. Differential Methylation of Ferroptosis-Related Genes

Filtering the CRC methylation dataset against FerrDb ferroptosis genes identified 55 DMPs across 38 genes. Thirty-five DMPs mapped to 24 ferroptosis-driver genes, comprising 33 hypomethylated and two hypermethylated loci. The remaining 20 DMPs mapped to 14 ferroptosis-suppressor genes, and all were hypomethylated. Thus, 53 of 55 ferroptosis-related DMPs (96.4%) showed tumour-associated hypomethylation.

Among hypomethylated driver DMPs, 16 (49%) were located in open-sea regions, 12 (36%) in CpG shores and five (15%) in CpG shelves. Sixteen (49%) were located in gene bodies, 10 (30%) within TSS1500, four (12%) in 3'UTRs, two (6%) in 5'UTRs and one (3%) in the first exon. The two hypermethylated driver probes were located in open-sea regions and gene bodies. For suppressor genes, 12 of 20 hypomethylated DMPs (60%) occurred in open sea, seven (35%) in shores and one (5%) in a shelf; nine (45%) were in gene bodies and five (25%) within TSS1500, with the remainder distributed across 5'UTR, 3'UTR, TSS200 and first-exon regions.

Several genes contained multiple DMPs. *DNAJB6* showed the greatest number among driver genes, with six loci (four hypomethylated and two hypermethylated), followed by *MAPK14* and *ZEB1*. Of the six *DNAJB6* DMPs identified in the tumour–adjacent-normal comparison, four met the exploratory survival threshold in at least one TCGA cohort: cg27023755, cg14213430, cg10401362 and cg02994253. The remaining two *DNAJB6* loci, cg12910268 and cg00114346, did not meet the $P<0.05$ exploratory threshold in either cohort. Among suppressor genes, *TP63* contained four hypomethylated DMPs, *ENPP2* contained three and *CAV1* contained two. A complete list of the significant DMPs identified in this study is provided in Supplementary Table S1.

3.2. Functional Enrichment of Differentially Methylated Ferroptosis Genes

For the ferroptosis-driver set, 21 genes were represented in the BioPlanet pathway analysis. A total of 134 pathways met the adjusted $P<0.05$ criterion. The ATF2 transcription factor network was the most significantly enriched pathway (5 genes; adjusted $P=8.5\times10^{-5}$), followed by autophagy regulation (4 genes; adjusted $P=1.16\times10^{-4}$). Other highly ranked pathways included the rapid glucocorticoid receptor pathway (3 genes; adjusted $P=1.40\times10^{-4}$) and activation of the AP-1 family of transcription factors (3 genes; adjusted $P=1.40\times10^{-4}$).

For the ferroptosis-suppressor set, 13 genes were represented in the BioPlanet pathway analysis. A total of 16 pathways met the adjusted $P<0.05$ criterion. The p53 signalling pathway was the most significantly enriched pathway (4 genes; adjusted

P=3.14×10⁻³), followed by the Keap1-NRF2 pathway (2 genes; adjusted P=6.66×10⁻³). Other highly ranked pathways included biosynthesis of unsaturated fatty acids (2 genes; adjusted P=1.07×10⁻²) and oxidative stress (2 genes; adjusted P=1.18×10⁻²). Collectively, these enrichment patterns highlight pathways involved in stress responses, autophagy, redox regulation and cell-death control that are relevant to ferroptosis. The enrichment results are summarised in Figure 2, while the complete results for ferroptosis-driver and ferroptosis-suppressor genes are provided in Supplementary Tables S2 and S3, respectively.

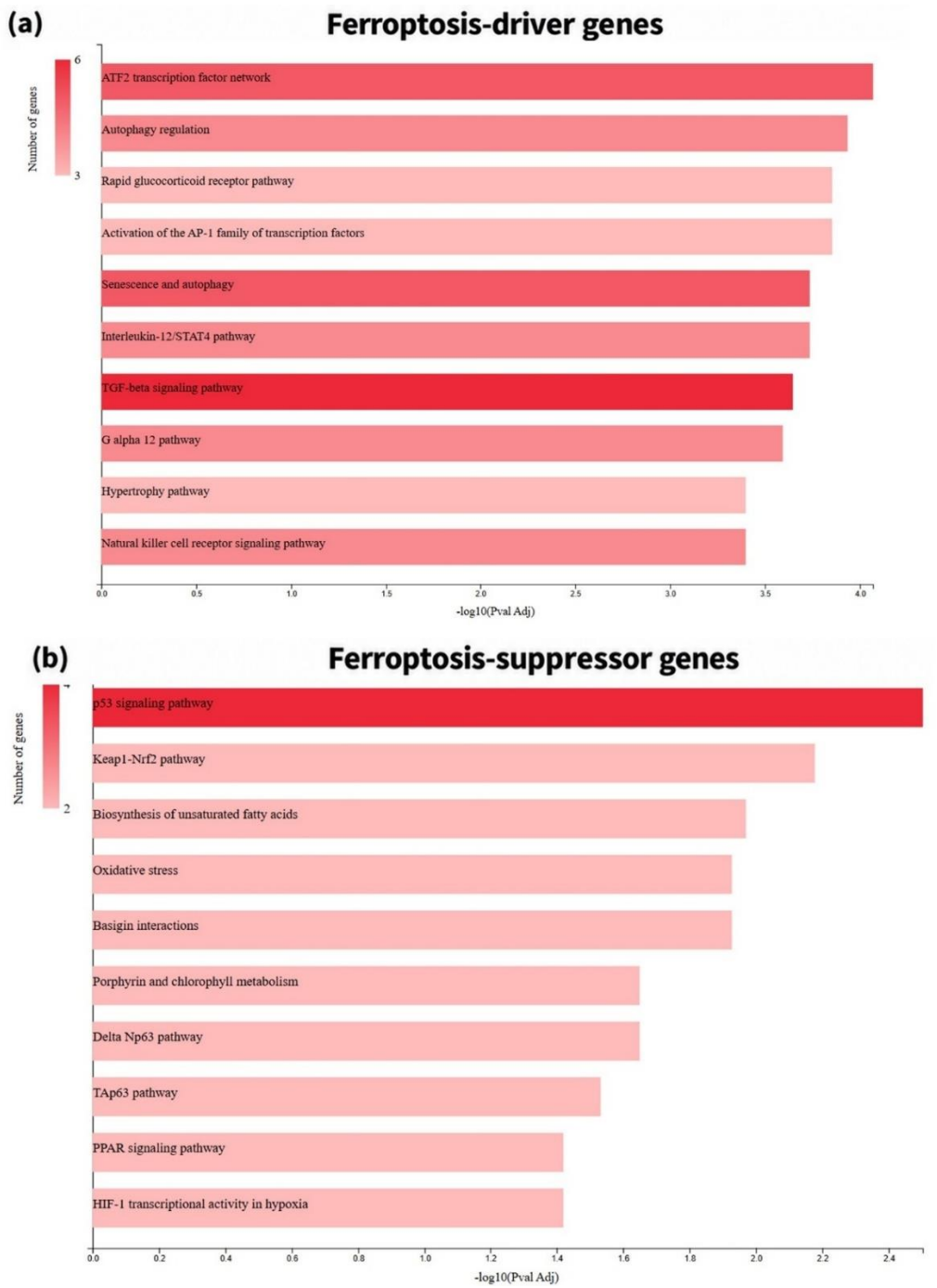


Figure 2. Functional enrichment of differentially methylated ferroptosis-related genes. (a) The 10 most significantly enriched pathways for ferroptosis-driver genes. (b) The 10 most significantly enriched pathways for ferroptosis-suppressor genes. The plots were generated using GeneCodis 4/BioPlanet.

3.3. Survival Associations

Seven of the 35 driver DMPs and one of the 20 suppressor DMPs met the predefined exploratory LR-test P<0.05 threshold for association with survival in TCGA-COAD, TCGA-READ or both datasets. The associated genes were *CDO1*, *DNAJB6*, *MAPK14*, *MAPK9* and *CAV1*. Eight unique DMPs generated nine statistically significant cohort-specific associations because *DNAJB6* cg27023755 was significant in both COAD and READ. Among the genes evaluated, *DNAJB6* contained the largest number of DMPs meeting the exploratory threshold, with four loci reaching LR-test P<0.05 in at least one TCGA cohort. However, since no multiple-testing correction was applied across the 55 DMPs evaluated in MethSurv, these survival findings should be interpreted as exploratory and hypothesis-generating. Probe-level results are presented in Table 1 and Figure 3.

Table 1. Ferroptosis-related DMPs associated with survival in TCGA-COAD and/or TCGA-READ.

Ferroptosis-related genes	Probes ID	Delta-beta value	LR test P value		Feature
			COAD	READ	
CDO1	cg18520851	-0.328269655	0.032	ns	Body
DNAJB6	cg27023755	-0.368088122	0.029	0.044	Body
DNAJB6	cg14213430	-0.263063181	0.027	ns	Body
DNAJB6	cg10401362	0.222855642	ns	0.021	Body
DNAJB6	cg02994253	-0.20870712	0.014	ns	3'UTR
MAPK14	cg26033870	-0.32280094	ns	0.045	Body
MAPK9	cg09663237	-0.200380969	ns	0.017	3'UTR
[#]*CAV1*	cg18498156	-0.23971705	0.043	ns	Body

[#]Ferroptosis-suppressor gene.ns = no statistically significant association reported for that dataset. LR, likelihood ratio.

3.4. Tissue-Discriminatory Potential of Ferroptosis-Related DMPs

ROC analysis performed within the discovery cohort identified strong apparent discrimination between CRC and paired adjacent-normal tissue among the leading ferroptosis-related DMPs. Because the same discovery dataset was used both to identify the DMPs and to calculate ROC curves, the resulting AUCs represent apparent rather than externally validated discrimination. Within this discovery set, *SNX4* cg27440834 showed the highest apparent AUC (AUC=0.9300; 95% CI 0.8834–0.9766; P<0.0001). The other top-ranked probes showed AUC values from 0.8975 to 0.9270, with P<0.0001 for all ten (Table 2). Driver-gene candidates included *DNAJB6*, *MAPK14*, *KRAS* and *ZEB1*, whereas *FADS2*, *TP63* and *CAV1* represented suppressor-gene candidates.

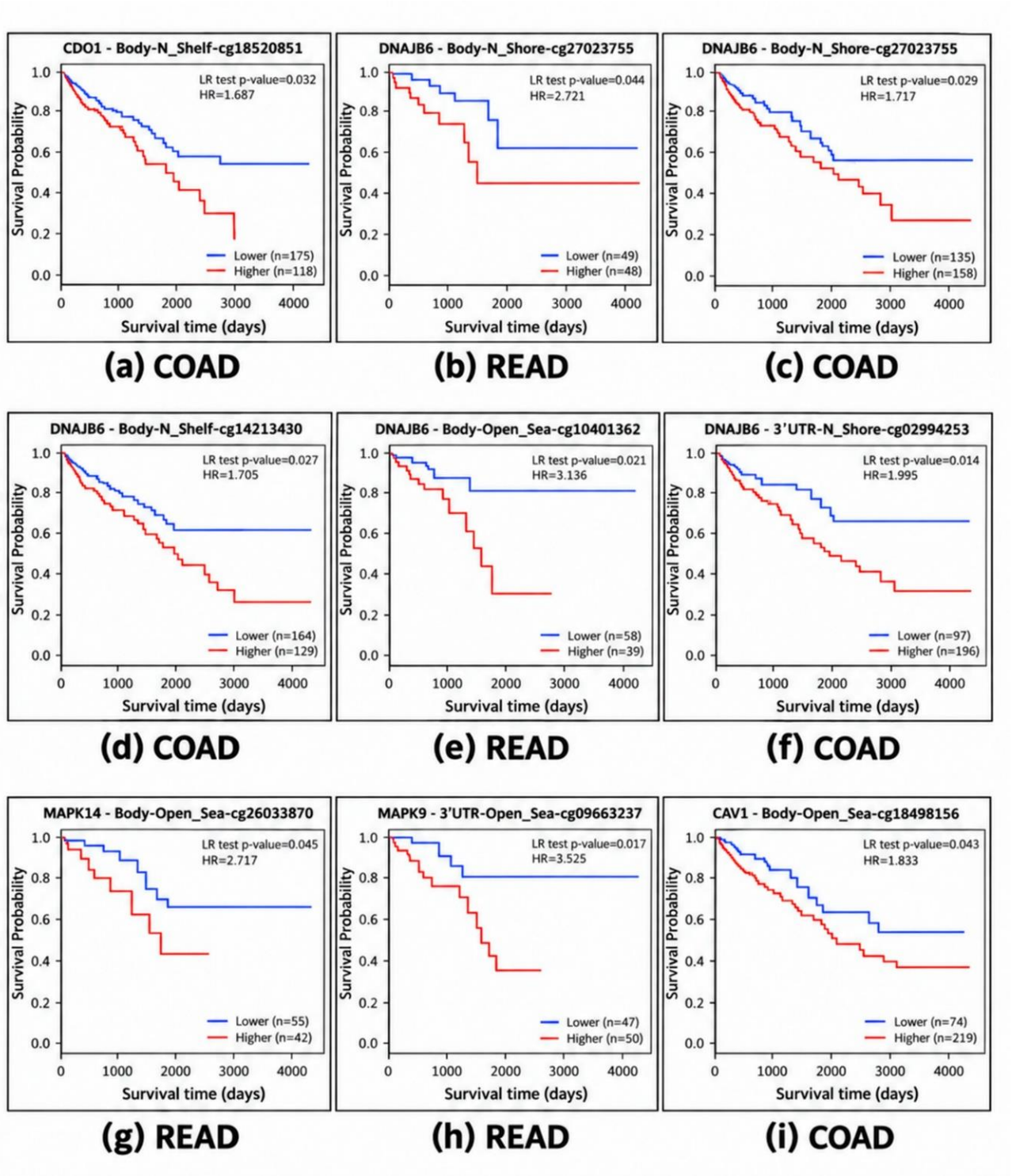


Figure 3. Kaplan–Meier survival plots for ferroptosis-related DMPs meeting the LR-test P<0.05 threshold in TCGA-COAD and/or TCGA-READ. COAD, colon adenocarcinoma; READ, rectal adenocarcinoma. Plots were generated using MethSurv.

Table 2. Ten ferroptosis-related DMPs with the highest ROC AUC values.

Gene	Probe	Ferroptosis Role	AUC	SE	95% CI	P value
SNX4	cg27440834	Driver	0.9300	0.02377	0.8834 to 0.9766	<0.0001
DNAJB6	cg27023755	Driver	0.9270	0.02436	0.8792 to 0.9747	<0.0001
MAPK14	cg16857825	Driver	0.9235	0.02641	0.8718 to 0.9753	<0.0001
MAPK14	cg26033870	Driver	0.9115	0.02666	0.8593 to 0.9638	<0.0001
KRAS	cg20341582	Driver	0.9088	0.02798	0.8539 to 0.9636	<0.0001
DNAJB6	cg14213430	Driver	0.9064	0.02927	0.8490 to 0.9637	<0.0001
FADS2	cg07999042	Suppressor	0.9036	0.03176	0.8414 to 0.9659	<0.0001
TP63	cg04483101	Suppressor	0.9026	0.03100	0.8419 to 0.9634	<0.0001
ZEB1	cg26365110	Driver	0.8995	0.03313	0.8346 to 0.9645	<0.0001
CAV1	cg18209470	Suppressor	0.8975	0.03127	0.8362 to 0.9588	<0.0001

AUC, area under the receiver operating characteristic curve; CI, confidence interval; SE, standard error.

4. Discussion

This study characterised the methylation profile of ferroptosis-related genes in CRC, identifying 55 DMPs across 38 genes with a strong predominance of tumour-associated hypomethylation. The findings connect epigenetic dysregulation to ferroptosis-related biology at three complementary levels: differential methylation, pathway enrichment and clinical association. Although these analyses are exploratory, the convergence of multiple signals in genes such as DNAJB6, together with the tissue-discriminatory potential of *SNX4* and other DMPs, supports further investigation of ferroptosis-associated methylation as a biomarker framework in CRC.

The marked predominance of hypomethylation among ferroptosis-related DMPs should be interpreted within the broader methylation landscape of this CRC cohort. In the original epigenome-wide analysis from which the present dataset was derived, 25,443 of 26,093 DMPs (97.5%) were hypomethylated, whereas only 650 were hypermethylated [20]. A similar pattern was observed in the present ferroptosis-focused analysis, in which 53 of 55 DMPs (96.4%) were hypomethylated. Thus, the predominance of hypomethylation among ferroptosis-related loci appears to largely reflect the broader genome-wide hypomethylation characteristic of this CRC methylome rather than a selective hypomethylation pattern unique to ferroptosis-related genes. Age-related heterogeneity may further contribute to the CRC methylation landscape, as recent evidence suggests that early-onset CRC can exhibit pronounced global and LINE-1 hypomethylation together with distinct alterations in broader

methylation architecture compared with late-onset disease [28]. The biological relevance of these findings therefore lies not simply in the direction of methylation change, but in the specific ferroptosis-related genes and loci affected and their convergence on functionally relevant pathways and clinical associations.

The genomic distribution of the identified DMPs is also important for their biological interpretation. A substantial proportion of the hypomethylated loci occurred in open-sea regions and gene bodies rather than within classical CpG-island promoters. The functional relationship between DNA methylation and gene expression is highly dependent on genomic context; while promoter-associated hypermethylation is commonly linked to transcriptional repression, methylation within gene bodies and distal regulatory regions may have more complex effects on transcription, alternative promoter usage and splicing [29]. Therefore, the predominance of hypomethylation observed in this study should not be interpreted as evidence of uniformly increased expression of the corresponding ferroptosis-related genes. Integration of CpG methylation with matched transcriptomic data will be required to determine whether the identified loci are associated with altered gene expression or other regulatory effects.

DNAJB6 was particularly notable because it contained the largest number of DMPs among ferroptosis-driver genes, comprising four hypomethylated and two hypermethylated loci, and several of these loci were associated with survival. Importantly, the survival-associated CpGs did not show a uniform direction of methylation change. Three loci, cg27023755, cg14213430 and cg02994253, were hypomethylated in CRC, whereas cg10401362 was hypermethylated. These CpGs also occurred in different genomic contexts, including gene-body, 3′UTR, CpG-shore, CpG-shelf and open-sea regions. This pattern suggests locus-specific epigenetic remodelling of *DNAJB6* rather than a simple gene-wide gain or loss of methylation. Consequently, *DNAJB6* may be better considered a locus-specific epigenetic candidate in CRC, for which individual CpG sites may have different regulatory and clinical implications. Direct CRC evidence linking methylation at cg27023755, cg14213430, cg10401362 or cg02994253 to *DNAJB6* expression is currently lacking; therefore, the transcriptional consequences of these individual loci cannot be inferred from methylation direction alone.

DNAJB6 encodes a member of the HSP40 molecular chaperone family and has been implicated in cellular protein homeostasis and cancer-related processes. Independent evidence also suggests that altered *DNAJB6* methylation may occur during colorectal neoplasia. In a genome-wide methylation study of colorectal adenoma and CRC, He *et al.*

identified cg26668151 within the *DNAJB6* gene body and open-sea region as a hypomethylated locus in colorectal adenoma [30]. Although cg26668151 is distinct from the *DNAJB6* CpGs identified in the present study, this observation supports the possibility that epigenetic dysregulation of *DNAJB6* can occur at multiple loci during colorectal tumour development. In CRC, overexpression of *DNAJB6* has been reported to promote invasion through IQGAP1/ERK-dependent signalling [31]. A direct relationship between *DNAJB6* and ferroptosis has also been reported in oesophageal squamous cell carcinoma, where *DNAJB6a* overexpression promoted ferroptotic processes involving glutathione depletion, reduced *GPX4* and increased lipid peroxidation [32]. The present findings do not establish that methylation changes at these individual *DNAJB6* loci alter gene expression or ferroptotic activity in CRC. Nevertheless, the coexistence of hypermethylated and hypomethylated loci, together with their survival associations, provides a rationale for CpG-specific validation and integration with *DNAJB6* expression in future studies.

The potential relevance of these methylation changes is further supported by growing evidence that epigenetic regulation can directly influence ferroptosis susceptibility in CRC. Recent studies indicate that this regulation extends beyond DNA methylation to other epigenetic mechanisms. Qiao *et al.* demonstrated that suppression of the m6A demethylase *FTO* promoted ferroptosis in CRC cells by reducing *SLC7A11* and *GPX4* expression through an m6A-dependent mechanism [33]. More recently, Qu *et al.* showed that PRMT5-mediated histone modifications contributed to ferroptosis resistance by suppressing *ALKBH5* and stabilising *SLC7A11* expression [34]. Together, these findings illustrate that multiple epigenetic layers can converge on key ferroptosis-regulatory pathways in CRC. However, locus-specific DNA methylation of ferroptosis-related genes remains comparatively less characterised, supporting the relevance of the present methylome-based analysis and the need to determine whether the identified CpG alterations have functional consequences for ferroptosis.

The pathway analysis further suggests that driver-gene methylation alterations intersect with the ATF2 transcriptional network. *ATF2* is a stress-responsive transcription factor with context-dependent tumour-promoting and tumour-suppressive functions [35]. In CRC models, loss or reduced activity of *ATF2* has been associated with enhanced tumour invasion and upregulation of the cancer driver *TROP2* [36]. In gastric cancer, *ATF2* has also been connected to sorafenib-induced ferroptosis through an ATF2-HSPH1-SLC7A11 axis [37]. However, an analogous ATF2-dependent ferroptosis mechanism has not yet been established in CRC. These observations provide a plausible biological context for the enrichment result, but the present study did not experimentally test *ATF2* pathway activity;

accordingly, the enrichment should be interpreted as hypothesis-generating rather than evidence of pathway activation or suppression.

Among ferroptosis-suppressor genes, p53 signalling was the most significantly enriched pathway, while Keap1-Nrf2 signalling was the second most significant. These pathways are mechanistically distinct but converge on the regulation of cellular redox homeostasis and ferroptosis susceptibility. p53 can modulate ferroptosis in a context-dependent manner through several downstream mechanisms, including regulation of cystine uptake, glutathione metabolism and lipid peroxidation [38,39]. This relationship is particularly relevant to CRC, in which *TP53* alterations are common and disruption of p53 signalling contributes to colorectal tumorigenesis [40]. Epigenetic alterations may further influence this pathway, as promoter and exon methylation changes affecting genes involved in colorectal carcinogenesis have been reported, [41] and broader epigenetic regulation upstream and downstream of p53 signalling has been described in CRC [42].

In contrast, the Keap1-NRF2 pathway represents a major antioxidant defence system that generally limits oxidative stress and lipid peroxidation by regulating glutathione metabolism, reactive oxygen species detoxification and iron homeostasis. Experimental evidence in CRC has shown that *NRF2* inhibition enhances ferroptosis and increases chemosensitivity, supporting an anti-ferroptotic role for *NRF2* signalling in this tumour context [43]. More broadly, *NRF2* has been recognised as a central regulator of ferroptosis through its control of antioxidant defence, iron handling and lipid-peroxidation pathways [44]. A recent CRC-focused review further highlighted *NRF2* as a ferroptosis gatekeeper through regulation of *GPX4*, *SLC7A11*, ferritin and ferroportin, reinforcing its role in maintaining redox balance and suppressing ferroptotic stress in colorectal cancer [45]. The concurrent enrichment of p53 and Keap1-NRF2 signalling therefore points towards redox regulation as a common biological theme among the differentially methylated ferroptosis-suppressor genes identified in this study, rather than representing two unrelated pathway alterations. Epigenetic disruption of components within these pathways could potentially shift the balance between antioxidant defence and ferroptotic stress in CRC; however, the present methylation data do not establish the direction or functional consequence of such regulation.

From a translational perspective, the ROC analysis identified several DMPs with strong tissue-level discrimination, with *SNX4* cg27440834 showing the highest performance (AUC=0.9300). This finding is noteworthy because direct evidence linking *SNX4* methylation to ferroptosis or CRC biomarker development remains limited. CRC-specific evidence for *SNX4* is also sparse; publicly available transcriptomic data confirm its

expression in colorectal tumours, although associations between *SNX4* expression and patient survival appear inconsistent across CRC cohorts [46]. *SNX4* is a sorting nexin involved in endosomal membrane trafficking and has been implicated in autophagosome assembly through regulation of ATG9A trafficking [47]. However, whether these cellular functions intersect with ferroptosis regulation in CRC is currently unclear, and the present data do not establish such a mechanistic relationship. Accordingly, cg27440834 should be regarded as a data-driven methylation candidate whose strong discriminatory performance warrants independent replication and functional annotation rather than as an established ferroptosis biomarker.

Other highly ranked DMPs occurred in *DNAJB6*, *MAPK14*, *KRAS*, *ZEB1*, *FADS2*, *TP63* and *CAV1*. Previous bioinformatic studies have likewise demonstrated prognostic value for ferroptosis-related gene signatures in CRC, [17,48] supporting the broader clinical relevance of ferroptosis-associated molecular alterations. However, the ROC analyses in the present study were performed using the same paired tissue dataset from which the DMPs were identified and therefore represent apparent rather than externally validated tissue-discriminatory performance. Moreover, discrimination between resected tumour and adjacent-normal mucosa should not be interpreted as evidence of clinical screening utility. Recent studies have demonstrated the feasibility of translating CRC-associated methylation alterations into non-invasive assays using plasma cell-free DNA and stool DNA [49]. More broadly, circulating molecular biomarkers such as plasma miRNA panels have also shown potential for minimally invasive CRC discrimination [50]. Therefore, the most promising loci identified here, including *SNX4* cg27440834, should next be evaluated in independent cohorts and in clinically accessible specimens such as plasma cfDNA or stool DNA to determine whether their tissue-discriminatory signals can be translated into non-invasive CRC detection biomarkers.

Several limitations should be considered when interpreting these findings. First, the discovery cohort comprised only 54 paired tumour and adjacent-normal samples, which limits generalisability and requires confirmation in larger independent cohorts. Second, the methylation profiles were generated from bulk tissue. CRC and adjacent-normal mucosa contain different proportions of epithelial, stromal and immune cells; therefore, some of the observed methylation differences may reflect variation in cellular composition rather than tumour-cell-intrinsic epigenetic alterations. Future studies incorporating cell-type deconvolution, purified cell populations or single-cell approaches would help distinguish these effects. Third, adjacent-normal mucosa should not necessarily be considered equivalent to healthy colon. Epigenetic field cancerisation has been demonstrated in morphologically

normal colorectal mucosa, including methylation alterations associated with adenomatous lesions and cancer-adjacent tissue [51]. Consequently, field effects may influence both the estimated tumour–normal methylation differences and the apparent tissue-discriminatory performance of individual DMPs. Finally, the HumanMethylation450K array interrogates approximately 485,000 predefined CpG sites and therefore provides broad but incomplete coverage of the human methylome. The present analysis also focused on individual DMPs rather than validating differentially methylated regions, and additional locus- or region-level alterations may therefore have been missed.

The survival analysis should likewise be interpreted as exploratory. Associations were identified using an LR-test $P<0.05$ threshold without correction for multiple comparisons, increasing the possibility of false-positive findings. In addition, patient groups were defined using MethSurv's data-driven "best cut-off point" procedure, which selects the threshold yielding the highest hazard ratio from several candidate dichotomisation methods. This optimisation may increase apparent survival separation and effect estimates; therefore, the observed associations require validation using prespecified cut-offs in independent cohorts. Functional validation was not performed, and potential determinants of DNA methylation such as age, lifestyle and genetic background were not modelled. Taken together, the identified DMPs should be regarded as prioritised candidates requiring replication in independent cohorts, regional and expression-level validation, and experimental confirmation before biological causality or clinical utility can be established.

5. Conclusion

Re-analysis of genome-wide methylation data identified 55 DMPs across 38 ferroptosis-related genes in CRC, with 53 of 55 loci showing tumour-associated hypomethylation. Differentially methylated ferroptosis-driver and ferroptosis-suppressor genes were enriched in biologically relevant pathways, including ATF2, p53 and Keap1-NRF2 signalling. Exploratory survival analysis prioritised DMPs in *CDO1*, *DNAJB6*, *MAPK14*, *MAPK9* and *CAV1*, with *DNAJB6* showing the greatest concentration of survival-associated loci, while *SNX4* cg27440834 demonstrated the strongest tissue-discriminatory potential. Collectively, these findings describe a locus-specific ferroptosis-related methylation pattern in CRC and prioritise CpG loci for further biological and translational investigation. Independent cohort replication, integration with gene-expression data and functional validation are required to determine the biological significance of these methylation alterations and their potential clinical utility. The next logical step is targeted bisulfite-based validation of the prioritised CpGs in an independent CRC cohort, ideally

coupled with matched RNA-expression analysis to determine whether the methylation changes are reproducible and functionally associated with transcription.

Supplementary Materials: Supplementary Table S1, differentially methylated probes associated with ferroptosis-related genes in colorectal cancer, including genomic annotation, delta-beta values and sample-level methylation beta values; Supplementary Table S2, functional enrichment results for differentially methylated ferroptosis-driver genes; Supplementary Table S3, functional enrichment results for differentially methylated ferroptosis-suppressor genes.

Author Contributions: Conceptualization, NSAM; methodology, FMK and NSAM; formal analysis, FMK and NSAM; investigation, FMK and NSAM; resources, NSAM; data curation, FMK; writing-original draft preparation, FMK and NSAM; writing-review and editing, NSAM, MRAZ, HA, LT-HT, JW-FL; supervision, NSAM. All authors have read and agreed to the published version of the manuscript.

Funding: This study was supported by the University Research Grant Scheme from the Universiti Kebangsaan Malaysia (GUP-2018-070).

Acknowledgments: During the preparation of this work, the authors used ChatGPT (OpenAI) to assist with language refinement, improvement of clarity and conciseness, and structural editing of selected sections of the manuscript, including the Introduction, Materials and methods, and Discussion. The tool was used to improve the presentation and readability of the manuscript and did not generate or modify the underlying experimental data. A representative prompt used was: "Revise this section to be concise, coherent, and suitable for a research article. Maintain a standard academic tone (balanced and precise)." Following the use of this tool, the authors critically reviewed and edited all generated content and accept full responsibility for the accuracy and integrity of the manuscript.

Conflicts of Interest: The authors declare no conflict of interest.

References

1. Morgan E, Arnold M, Gini A, *et al.* Global burden of colorectal cancer in 2020 and 2040: incidence and mortality estimates from GLOBOCAN. Gut 2023; 72(2): 338–344. doi: 10.1136/gutjnl-2022-327736.
2. Muhamad NA, Ma'amor NH, Rosli IA, *et al.* Colorectal cancer survival among Malaysia population: data from the Malaysian National Cancer Registry. Frontiers in Oncology 2023; 13. doi: 10.3389/fonc.2023.1132417.
3. Yunos R-IM, Mutalib N-SA, Khor SS, *et al.* Whole exome sequencing identifies genomic alterations in proximal and distal colorectal cancer. Progress In Microbes & Molecular Biology 2019; 2(1). doi: 10.36877/pmmb.a0000036.
4. Lao V, Grady W. Epigenetics and colorectal cancer. Nature Reviews Gastroenterology & Hepatology 2011; 8(12): 686–700. doi: 10.1038/nrgastro.2011.173.
5. Ishak M, Baharudin R, Mohamed Rose I, *et al.* Genome-Wide Open Chromatin Methylome Profiles in Colorectal Cancer. Biomolecules 2020; 10(5): 719. doi: 10.3390/biom10050719.
6. Ishak M, Baharudin R, Tan LT-H, *et al.* Landscape Of HOXA Genes Methylation in Colorectal Cancer. Progress In Microbes & Molecular Biology 2020; 3(1). doi: 10.36877/pmmb.a0000085.
7. Abu N, Rus Bakarurraini NAA, Nasir SN, *et al.* Methylation Profile of Cancer Testis Antigens in Colorectal Cancer. Iranian Journal of Immunology 2023; 20(1). doi: 10.22034/iji.2023.92600.2171.
8. Zabidi NAN, Baharudin R, Rus Bakarurraini NQ, *et al.* Investigating DNA Methylation of Solute Carrier Genes in Colorectal Cancer: A Comprehensive Analysis Using Microarray and Bioinformatics Tools. Progress In Microbes & Molecular Biology 2023; 6(1). doi: 10.36877/pmmb.a0000393.

9. Norhisan NN, Baharudin R, Bakarurraini NQR, *et al.* Decoding the Methylation Patterns of ABC Transporters in Colorectal Cancer. Progress In Microbes & Molecular Biology 2024; 7(1). doi: 10.36877/pmmb.a0000450.
10. Moore LD, Le T, Fan G. DNA Methylation and Its Basic Function. Neuropsychopharmacology 2013; 38(1): 23–38. doi: 10.1038/npp.2012.112.
11. Omari NE, Bakrim S, Bakha M, *et al.* DNA Methylation: Its Role and Interaction with Epigenetic Modifications in Cancer. Progress In Microbes & Molecular Biology 2025; 8(1). doi: 10.36877/pmmb.a0000458.
12. Dixon SJ, Lemberg KM, Lamprecht MR, *et al.* Ferroptosis: an iron-dependent form of nonapoptotic cell death. Cell 2012; 149(5): 1060–1072. doi: 10.1016/j.cell.2012.03.042.
13. Mou Y, Wang J, Wu J, *et al.* Ferroptosis, a new form of cell death: opportunities and challenges in cancer. Journal of Hematology & Oncology 2019; 12: 34. doi: 10.1186/s13045-019-0720-y.
14. Li J, Cao F, Yin HL, *et al.* Ferroptosis: past, present and future. Cell Death & Disease 2020; 11(2): 88. doi: 10.1038/s41419-020-2298-2.
15. Liang X, You Z, Chen X, *et al.* Targeting ferroptosis in colorectal cancer. Metabolites 2022; 12(8): 745. doi: 10.3390/metabo12080745.
16. Kong J, Lyu H, Ouyang Q, *et al.* Insights into the roles of epigenetic modifications in ferroptosis. Biology (Basel 2024; 13(2): 122. doi: 10.3390/biology13020122.
17. Liu R, Wang Y, Bu J, *et al.* Construction and validation of novel ferroptosis-related risk score signature and prognostic prediction nomogram for patients with colorectal cancer. International Journal of Medical Sciences 2024; 21(6): 1103–1116. doi: 10.7150/ijms.91446.
18. Lye K-L, Tan LT-H, Yap H-M. Insight of microRNA role in Colorectal Cancer. Progress In Microbes & Molecular Biology 2020; 3(1). doi: 10.36877/pmmb.a0000083.
19. Zhao Y-P, Liu J-L, Wang S, *et al.* Role of non-coding RNA-regulated ferroptosis in colorectal cancer. Cell Death Discovery 2025; 11(1): 315. doi: 10.1038/s41420-025-02606-6.
20. Baharudin R, Ishak M, Muhamad Yusof A, *et al.* Epigenome-Wide DNA Methylation Profiling in Colorectal Cancer and Normal Adjacent Colon Using Infinium Human Methylation 450K. Diagnostics 2022; 12(1): 198. doi: 10.3390/diagnostics12010198.
21. Tian Y, Morris TJ, Webster AP, *et al.* ChAMP: updated methylation analysis pipeline for Illumina BeadChips. Bioinformatics 2017; 33(24): 3982–3984. doi: 10.1093/bioinformatics/btx513.
22. Johnson WE, Li C, Rabinovic A. Adjusting batch effects in microarray expression data using empirical Bayes methods. Biostatistics 2007; 8(1): 118–127. doi: 10.1093/biostatistics/kxj037.
23. Dedeurwaerder S, Defrance M, Calonne E, *et al.* Evaluation of the Infinium Methylation 450K technology. Epigenomics 2011; 3(6): 771–784. doi: 10.2217/epi.11.105.
24. Zhou N, Yuan X, Du Q, *et al.* FerrDb V2: update of the manually curated database of ferroptosis regulators and ferroptosis-disease associations. Nucleic Acids Research 2023; 51(D1): D571–D582. doi: 10.1093/nar/gkac935.
25. Carmona-Saez P, Chagoyen M, Tirado F, *et al.* GENECODIS: a web-based tool for finding significant concurrent annotations in gene lists. Genome Biology 2007; 8(1): R3. doi: 10.1186/gb-2007-8-1-r3.
26. Garcia-Moreno A, López-Domínguez R, Villatoro-García JA, *et al.* Functional Enrichment Analysis of Regulatory Elements. Biomedicines 2022; 10(3): 590. doi: 10.3390/biomedicines10030590.

27. Modhukur V, Iljasenko T, Metsalu T, *et al.* MethSurv: A Web Tool to Perform Multivariable Survival Analysis Using DNA Methylation Data. Epigenomics 2018; 10(3): 277–288. doi: 10.2217/epi-2017-0118.
28. Henry F, Uddin MAR, Ser H-L, *et al.* Microbial and Molecular Drivers of early-Onset Colorectal Cancer. Progress In Microbes & Molecular Biology 2026; 9(1). doi: 10.36877/pmmb.a0000654.
29. Jones PA. Functions of DNA methylation: islands, start sites, gene bodies and beyond. Nature Reviews. Genetics 2012; 13(7): 484–492. doi: 10.1038/nrg3230.
30. He C, Huang Q, Zhong S, *et al.* Screening and identifying of biomarkers in early colorectal cancer and adenoma based on genome-wide methylation profiles. World Journal of Surgical Oncology 2023; 21: 312. doi: 10.1186/s12957-023-03189-1.
31. Zhang TT, Jiang YY, Shang L, *et al.* Overexpression of DNAJB6 promotes colorectal cancer cell invasion through an IQGAP1/ERK-dependent signaling pathway. Molecular Carcinogenesis 2015; 54(10): 1205–1213. doi: 10.1002/mc.22194.
32. Jiang B, Zhao Y, Shi M, *et al.* DNAJB6 promotes ferroptosis in esophageal squamous cell carcinoma. Digestive Diseases and Sciences 2020; 65(7): 1999–2008. doi: 10.1007/s10620-019-05929-4.
33. Qiao Y, Su M, Zhao H, *et al.* Targeting FTO induces colorectal cancer ferroptotic cell death by decreasing SLC7A11/GPX4 expression. Journal of experimental & clinical cancer research: CR 2024; 43(1): 108. doi: 10.1186/s13046-024-03032-9.
34. Qu S, Feng B, Xing M, *et al.* PRMT5 K240lac confers ferroptosis resistance via ALKBH5/SLC7A11 axis in colorectal cancer. Oncogene 2025; 44(32): 2814–2830. doi: 10.1038/s41388-025-03457-2.
35. Huebner K, Prochazka J, Monteiro AC, *et al.* The activating transcription factor 2: an influencer of cancer progression. Mutagenesis 2019; 34(5–6): 375–389. doi: 10.1093/mutage/gez041.
36. Huebner K, Erlenbach-Wuensch K, Prochazka J, *et al.* ATF2 loss promotes tumor invasion in colorectal cancer cells via upregulation of cancer driver TROP2. Cellular and Molecular Life Sciences 2022; 79(8): 423. doi: 10.1007/s00018-022-04445-5.
37. Xu X, Li Y, Wu Y, *et al.* Increased ATF2 expression predicts poor prognosis and inhibits sorafenib-induced ferroptosis in gastric cancer. Redox Biology 2023; 59: 102564. doi: 10.1016/j.redox.2022.102564.
38. Hernández Borrero L, El-Deiry W. Tumor suppressor p53: biology, signaling pathways, and therapeutic targeting. Biochimica et Biophysica Acta Reviews on Cancer 2021; 1876(1): 188556. doi: 10.1016/j.bbcan.2021.188556.
39. Xu R, Wang W, Zhang W. Ferroptosis and the bidirectional regulatory factor p53. Cell Death Discovery 2023; 9: 197. doi: 10.1038/s41420-023-01517-8.
40. Nakayama M, Oshima M. Mutant p53 in colon cancer. Journal of Molecular Cell Biology 2019; 11(4): 267–276. doi: 10.1093/jmcb/mjy075.
41. Molnar B, Galamb O, Peterfia B, *et al.* Gene promoter and exon DNA methylation changes in colon cancer development-mRNA expression and tumor mutation alterations. BMC Cancer 2018; 18: 659. doi: 10.1186/s12885-018-4609-x.
42. Tomicic MT, Dawood M, Efferth T. Epigenetic alterations upstream and downstream of p53 signaling in colorectal carcinoma. Cancers (Basel) 2021; 13(16): 4072. doi: 10.3390/cancers13164072.

43. Huang Y, Yang W, Yang L, *et al.* Nrf2 inhibition increases sensitivity to chemotherapy of colorectal cancer by promoting ferroptosis and pyroptosis. Scientific Reports 2023; 13(1): 14359. doi: 10.1038/s41598-023-41490-x.
44. Jiang X, Yu M, Wang W-K, *et al.* The regulation and function of Nrf2 signaling in ferroptosis-activated cancer therapy. Acta Pharmacologica Sinica 2024; 45(11): 2229–2240. doi: 10.1038/s41401-024-01336-2.
45. Abdelgawwad El-Sehrawy AAM, Al-dulaimi AA, Alkhathami AG, *et al.* NRF2 as a ferroptosis gatekeeper in colorectal cancer: implications for therapy. Naunyn-Schmiedeberg's Archives of Pharmacology 2025; 398(12): 16479–16506. doi: 10.1007/s00210-025-04324-3.
46. Uhlen M, Zhang C, Lee S, *et al.* A pathology atlas of the human cancer transcriptome. Science 2017; 357(6352): eaan2507. doi: 10.1126/science.aan2507.
47. Antón Z, Betin VMS, Simonetti B, *et al.* A heterodimeric SNX4--SNX7 SNX-BAR autophagy complex coordinates ATG9A trafficking for efficient autophagosome assembly. Journal of Cell Science 2020; 133(14): jcs246306. doi: 10.1242/jcs.246306.
48. Hu D, Zhou Z, Wang J, *et al.* Screening of ferroptosis-related genes with prognostic effect in colorectal cancer by bioinformatic analysis. Frontiers in Molecular Biosciences 2022; 9: 979854. doi: 10.3389/fmolb.2022.979854.
49. Long Z, Gao Y, Han Z, *et al.* Discovery and Validation of Methylation Signatures in Circulating Cell-Free DNA for the Detection of Colorectal Cancer. Biomolecules 2024; 14(8): 996. doi: 10.3390/biom14080996.
50. Mohamed SS, Ahmad A, Mutalib NSA, *et al.* A Panel of Three MicroRNA Signatures as a Potential Biomarker for CRC Screening Based on Stages and Functional Prediction Using Bioinformatic Analysis. Progress In Microbes & Molecular Biology 2023; 6(1). doi: 10.36877/pmmb.a0000343.
51. Yates J, Schaufelberger H, Steinacher R, *et al.* DNA-methylation variability in normal mucosa: a field cancerization marker in patients with adenomatous polyps. Journal of the National Cancer Institute 2024; 116(6): 974–982. doi: 10.1093/jnci/djae016.

Author(s) shall retain the copyright of their work and grant the Journal/Publisher right for the first publication with the work simultaneously licensed under:

Creative Commons Attribution-NonCommercial 4.0 International (CC BY-NC 4.0). This license allows for the copying, distribution and transmission of the work, provided the correct attribution of the original creator is stated. Adaptation and remixing are also permitted.